Journal of the Korean Nuclear Society
Volume 26, Number 1, March 1994

A Semi-Empirical Correlation for an Adiabatic Interfacial Friction Factor

Ho-Yun Nam and Moon-Hyun Chun
Korea Advanced Institute of Science and Technology
(Received December 2, 1993)

단열 계면 마찰계수에 대한 준 실험식

남호윤 · 전문헌
한국과학기술원
(1993. 12. 2 접수)

Abstract

A semi-empirical correlation has been developed for adiabatic interfacial friction factors in a long horizontal air-water countercurrent stratified flow conditions. Using a pipe and duct test sections, a series of experiments have been conducted varying non-dimensional water depth and flow rates of air. On the basis of simultaneous measurements of the main flow parameters in a horizontal pipe and a duct, a semi-empirical correlation for the interfacial friction factor in a stratified flow regime has been developed employing a new concept of surface roughness in wavy flow. A total of 201 data points, including 15 concurrent pipe flow test data of others, have been used in the present analysis. A comparison between the data and the predictions of the present correlation shows that the agreement is within ±30%.

요 약

긴 수평관에서 공기와 물의 역성층류시 적용할 수 있는 단열계면 마찰계수에 대한 준 실험식을 개발하였다. 둥근관과 사각관으로 된 단열 역성층류 실험장치를 사용하여 물의 수위 및 공기의 속도를 변화시키면서 일련의 실험을 수행하였다. 수평으로 된 원형 및 사각형 실험관속으로 흐르는 유체의 주요 유동변수들을 동시에 측정한 실험치들과 계면이 물결파에 의해 거칠어진다는 새로운 개념을 도입하여 성층류영역의 계면마찰 계수에 대한 준 실험식을 개발하였다. 이 해석에는 다른 연구자들의 병류실험치 15개를 포함하여 총 201개의 실험치들을 사용하였다. 이 실험치들과 여기서 제안한 준 실험식의 예측치와 비교하면 오차 범위는 ±30% 정도이다.

1. Introduction

The interfacial friction factor is one of the key flow parameters which is essential in the analysis of two-phase flow and system responses such as (1) the condensation-induced waterhammer (CIWH) in a long horizontal pipe, (2) two-phase flow pressure drops, and (3) flow transition criteria including the

flooding point.

A number of attempts have been made to correlate the variation of the interfacial friction factor or effective interface roughness with other flow parameters. However, with the exception of the works reported by Kim et al. [1] and Lee and Bankoff [2] most of the existing studies on the interfacial friction factor (f_i) were performed almost exclusively for concurrent flow conditions.

The most widely used existing correlations for interfacial friction factor are summarized in Table 1: Cheremisinoff and Davis [3] attempted to account for the effect of interfacial waves on f_i and proposed two formulas, one for small amplitude waves and the other for roll waves based on the measurements of Miya et al. [4]. Lee and Bankoff [2] obtained an empirical correlation of f_i for roll-wave regime (near-flooding) in nearly horizontal steam-water countercurrent flow. Kim et al. [1] also give an adiabatic interfacial friction factor for a nearly horizontal countercurrent steam-saturated water flow in rectangular channels (aspect ratio = 5). Kowalski [5], on the other hand, made direct measurements of the Reynolds shear stress in the gas for horizontal stratified flow in a pipe and recommended two different equations for the interfacial friction factor for smooth and wavy surfaces, respectively. Andritsos and Hanratty [6] proposed two empirical correlations of the measurements of f_i/f_g employing the gas phase velocity as a criterion.

From the above brief summary of existing correlations for f_i, following observations can be made:

(1) Most of the existing correlations of f_i consist of two equations which are applicable for different flow regimes depending on the flow conditions.

(2) Each correlation has different criteria for flow regime transition.

With a few exception, the main finding from these earlier studies has been that the interfacial friction factor or interface roughness is a direct function of the liquid film thickness and Reynolds number.

The main objective of the present work is to determine the adiabatic interfacial friction factor in horizontal air-water countercurrent stratified flow conditions based on the simultaneous measurements of main flow parameters such as pressure drop, flow velocities of air and water, and height of liquid in a horizontal pipe and a duct. In addition, an outline of the procedure used to derive a semi-empirical correlation for air-water interface friction factor f_i in a stratified flow by making an analogy between the effect of surface roughness on f_g in a pipe flow and the effect of gas-water interface roughness on f_i in a wavy flow along with the present experimental data is presented here.

2. Experimental Method

A schematic diagram of experimental apparatus is shown in Fig.1. It consists of an air-water fluid system where the water and air circuits are combined to form a countercurrent flow at the horizontal test section. Major components of the experimental facility are: (1) water surge tank, (2) air compressor, (3) two horizontal test sections, one is made of transparent acrylic pipe (0.05m inside diameter and 8.28m in length) and the other is a duct ($0.1 \times 0.1m$ cross section and 7.98 in length), and (4) associated sensors and devices to measure flow rates of air and water and the pressure drop.

The water surge tank is installed to provide enough head for water flowing by gravity. The inner vessel installed inside the water surge tank maintains constant head of water to prevent water flowing in from riffling. The two reservoirs located at both sides of the test section maintain steady state flow conditions and absorb waves generated in the test section.

The volume flow rate of air was measured by two pitot tube type flowmeters (OMEGA models FPT−6310 and FPT−6320) with differential pressure transducers installed in series in the air line. The volume flow rate of water was calculated by

Table 1. Empirical Correlations for Interfacial Friction Factor

Authors	Geometry	Correlation	
Cheremisinoff and Davis (1979) [3]	countercurrent duct flow	$f_i = 0.0142$	(for small-amplitude waves)
		$f_i = 0.0008 + 2\times10^{-5}\, Re_l$	(for roll waves)
		$Re_l = \frac{V_{ls}}{vl}\frac{\pi D^2}{4S_i}$	
Lee and Bankoff (1983) [2]	countercurrent duct flow	$f_i = 0.012 + 5.174\times10^{-4}\,\frac{R_{e,g}-R^*_{e,g}}{1000}$,	(for $R_{e,g} < R^*_{e,g}$)
		$f_i = 0.012 + 2.694\times10^{-4}\,(\frac{R_{e,l}}{1000})^{1.534}\,\frac{R_{e,g}-R^*_{e,g}}{1000}$,	(for $R_{e,g} > R^*_{e,g}$)
		$R^*_{e,g} = 1.837\times10^5\, R_{e,l}^{-0.184}$	
Kowalski (1984) [5]	concurrent pipe flow	$f_i = 0.96(R^+_{e,g})^{-0.52}$	(for smooth surface)
		$f_i = 7.5\times10^{-5}(1-\alpha)^{-0.25}\, R_{e,g}^{-0.3}\, R_{e,l}^{0.83}$	(for wavy surface)
		$R^+_{e,g} = \frac{V_{gs}D}{v_g}$, $R_{e,g} = \frac{V_gD}{V_g}$, $R_{e,l} = \frac{V_lD}{V_l}$	
Kim et al. (1985) [1]	countercurrent duct flow	$f^{ia} = 0.560\times10^{-5}\, R_{e,l} + 0.084$	
Andritsos and Hanratty (1987) [6]	concurrent pipe flow	$\frac{f_i}{f_g} = 1.$	(for $V_{gs} \le V_{gs,t}$)
		$\frac{f_i}{f_g} = 1 + 15(\frac{H_l}{D})^{0.5}(\frac{V_{gs}}{V_{gs,t}} - 1)$	(for $V_{gs} > V_{gs,t}$)
		$V_{gs,t} = 5(\frac{\rho_{go}}{\rho_g})^{1/2}$, $f_g = 0.046\, R_e^{-0.2}$	

measuring the time it takes to fill a 22.5 ℓ water receiver via a water outlet. The pressure drop of the air between both ends of the test section was measured by one of the two differential pressure transducers (3″ H_2O and 10″ H_2O) installed in parallel depending on the experimental range. The temperatures of water and air were also measured by means of two thermocouples installed at the water surge tank and the air reservoir, respectively. The measured temperature range was 9~16℃ in the present work. Measurements of the water depth were made by the rulers attached to the test section (at 7 locations for the pipe test and 11 locations for the duct test). For each preset experimental conditions, the measurement was repeated five times to obtain an average value.

The velocity of a surface wave, on the other hand, was obtained by measuring the average traveling time of the surface wave between the known distance of the present test sections.

A series of experiments have been conducted varying the nondimensional water depth (H_ℓ/D) from 104 to 0.785 and for various combinations of air and water flow rates. The range of superficial water velocity was 0.02~0.12m/s in the pipe test and 0.053~0.26m/s in the duct test. The range of superficial air velocity, on the other hand, was 0.35~5.0m/s in the pipe test and 0.2~7.5m/s in the duct test. The actual air flow velocity was less than 13m/s, and all the flow regimes of air were fully turbulent flow. A

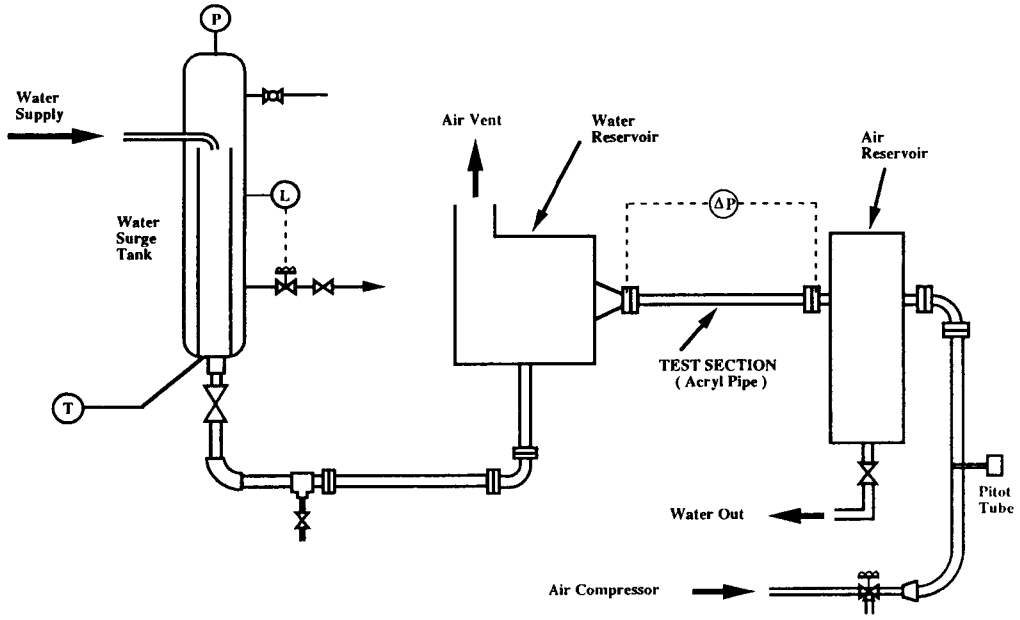

Fig. 1. Schematic Diagram of Experimental Apparatus

total of 201 data, i.e., 186 data points from the present countercurrent flow test and 15 from the concurrent pipe flow experimental data reported by others, have been used in the present analysis.

3. Functional Form For f_i

An insight into a proper functional form for f_i applicable for a horizontal air-water countercurrent stratified flow can be obtained from the review of existing correlations for f_g and the general theory of surface wave.

3.1. Existing Correlations for f_g that Include Relative Wall Roughness

Among the various models that have been proposed for f_g, the most simple approximate equation which includes the effect of surface roughness in the Blasius formula is given by Altshul [7]

$$f_g = \frac{1}{4}\left[0.11\left(\varepsilon_w^* + \frac{68}{Re_g}\right)^{1/4}\right] \quad (1)$$

Equation (1) is applicable for a stabilized flow and the region of purely turbulent flow in commercial circular tubes. When the surface roughness is dominant, Eq.(1) reduces to

$$f_g = \frac{1}{4}[0.11\ (\varepsilon_w^*)^{1/4}] \quad (2)$$

where

$$\varepsilon_w^* = \varepsilon_w/D_h$$

3.2. Relative Roughness of the Gas-Liquid Interface

Both from the descriptions on the surface wave behaviors reported by earlier workers [8, 9] and some intuitive reasoning from the qualitative relationships between the gas flow rate, the amplitudes of the waves and the wavelengths, a general expression for ε_i can be derived as follows:

(1) At relatively low gas velocity region (〈5*m*/s), the wave number (k) is proportional to the power between -1 and -2 of the gas velocity (i.e., k~ $1/V_g^{1\sim2}$), *whereas the wave amplitude* (η_o) *varies*

according to the square of the gas velocity (i.e., $\eta_o \sim V_g^2$). Therefore, the gas-water interface roughness (ε_i) at low gas velocity can be expressed as

$$\varepsilon_i \simeq k\eta_o \sim V_g^{0\sim 1} \quad \text{(At low gas velocity)} \tag{3}$$

(2) As the gas velocity becomes higher, the wave number begins to vary according to the first power of V_g. At the highest gas velocity, both the wave number and the wave amplitude become eventually proportional to V_g^2. For this case, therefore, ε_i can be expressed as

$$\varepsilon_i \simeq k\eta_o \sim V_g^4 \quad \text{(At the highest gas velocity)} \tag{4}$$

(3) From the analysis and curve fitting of the wave characteristics data obtained in the present experiment, in particular, it is found that the minimum value of the exponent of the gas velocity is approximately 0.8 when V_g reaches close to zero.

From the above qualitative relationships, it may be inferred that ε_i can be expressed, in general, as

$$\varepsilon_i \simeq V_g^{(c+Z)} \tag{5}$$

where $c+Z \leq 4$. That is, Eq.(5) states that ε_i varies as $V_g^{(c+Z)}$ where Z is also a function of the gas velocity.

Since $k\eta_o$ is a dimensionless quantity, Eq.(5) is also transformed into a non-dimensional form as follows:

$$\varepsilon_i^* \simeq (bX)^{(c+X)} \tag{6}$$

where $c+X \leq 4$, and ε_i^* is defined as

$$\varepsilon_i^* \equiv \frac{\varepsilon_i}{D_h} \tag{7}$$

In Eq.(6) X is a is a dimensionless velocity.

3.3. Assumptions and Analogy Between ε_w^* and ε_i^*

The tube roughness characterized by the ratio of the depth of surface protrusions to the tube diameter (i.e., $\varepsilon_w^* = \varepsilon_w/D_h$), may increase the effective friction factor. In Moody's chart [10], the effect of the roughness depends on the pipe diameter.

Similarly, the air-water interface roughness can be represented by the relative roughness of the interface (i.e., $\varepsilon_i^* = \varepsilon_i/D_h$). The relative roughness of the interface, ε_i^*, on the other hand, can be described in terms of the wave number (k) and wave amplitude (η_o) obtained from the theory of surface wave. As in the case of the ε_w^*, the interface roughness characterized by ε_i^* may increase the effective interfacial friction factor.

Based on the above observations, following assumptions are made here:

(1) The relative roughness of the air-water interface (ε_i^*) in a stratified flow acts on the f_i analogously to the relative wall roughness (ε_w^*) that gives rise to a gas-to-wall friction factor (f_g) whose value depends on ε_w/D_h and Reynolds number in a pipe flow.

(2) The relative roughness of the air-water interface (ε_i^*) can be described in terms of wave number (k) and wave amplitude (η_o) obtained from the theory of surface wave as follows:

$$\varepsilon_i^* \simeq \kappa\, \eta_o \tag{8}$$

3.4. Functional Form of the Present Correlation

Using the above assumptions, and substituting ε_i^* given by Eq.(6) into Eq.(2) for ε_w^* and replacing f_g by f_i, the final functional form for f_i can be obtained:

$$f_i = a\,(bX)^{(c+X)/4} \tag{9}$$

and

$$c + X \leq 4 \ .$$

The constants a, b, and c, and the dimensionless velocity X in Eq.(9) can be determined using the combined method of dimensional analysis, curve fitting of experimental data, and a numerous repetition of trial and error.

4. Analysis of Experimental Data and Final Correlation for f_i

4.1. An Expression for f_i from the Momentum Equation

The momentum balance for fully developed air-water countercurrent stratified flow for the gas phase is given by

$$A_g\left(\frac{dP}{dx}\right) = \tau_g S_g + \tau_i S_i \quad (10)$$

As can be seen in Fig.2, Eq.(10) represents a balance between the pressure forces on the gas space and the resisting stresses at the gas-wall boundary, τ_g, and at the gas-liquid interface, τ_i. The stresses τ_g and τ_i can be expressed in terms of friction factors

$$\tau_g = \frac{1}{2} f_g \rho_g V_g^2 \quad (11)$$

$$\tau_i = \frac{1}{2} f_i \rho_g V_r^2 \quad (12)$$

where V_g is the mean air velocity and V_r is the relative velocity defined by

$$V_r = V_g \pm V_l \quad (13)$$

In Eq.(13), the positive sign is for air-water countercurrent flow and the negative sign is for concurrent flow.

Assuming that the gas-phase pressure drop is linearly proportional to the length of the pipe (or duct), Eq.(10) can be rewritten as

$$A_g\left(\frac{\Delta P}{L}\right) = \tau_g S_g + \tau_i S_i \quad (14)$$

Substituting Eqs.(11) and (12) into Eq.(14) and solving for f_i

$$f_i = \frac{1}{S_i V_r^2}\left(\frac{2 A_g \Delta P}{\rho_g L} - f_g S_g V_g^2\right) \quad (15)$$

The gas-to-wall friction factor, f_g, to be used in Eq. (15) has been determined from the present experiment performed with air only and the definition of the skin-friction coefficient C_f:

$$C_f = 4 f_g = \frac{\Delta P}{\left(\frac{L}{D}\right)\left(\frac{\rho_g V_g^2}{2}\right)} \quad (16)$$

An empirical correlation for f_g, that is applicable for the present test conditions, has been obtained by means of curve-fitting as shown in Fig.3. For both pipe and duct test sections, the empirical correlation for f_g is given by

$$f_g = 0.0605\, R_{e,g}^{-0.22} \quad \text{(for pipe)} \quad (17a)$$

$$f_g = 0.0650\, R_{e,g}^{-0.22} \quad \text{(for duct)} \quad (17b)$$

for gas Reynolds numbers between 3×10^4 and 6×10^4. The Blasius relation shown in Fig.3 is given by

$$f_g = \frac{C_f}{4} = \frac{0.316}{4} R_{e,g}^{-0.25} = 0.079\, R_{e,g}^{-0.25} \quad (18)$$

Equation (18) gives the turbulent friction factor for a smooth tube and applicable for $R_{e,g} < 30{,}000$.

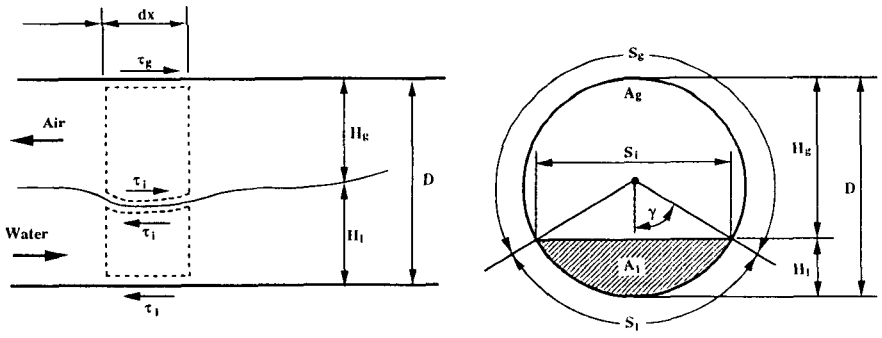

(a) Control Volumes for Mass, Momentum, and Energy Balances

(b) Stratified Flow Geometry in a Pipe

Fig. 2. Model Used for Analysis of Interfacial Friction Factor

As can be seen in Fig.3, Eq.(17a) gives slightly smaller values of f_g than the Blasius relation when $R_{e,g}$ is less than 10^4, whereas Eq.(17a) predicts slightly larger values of f_g than Eq.(18) for $R_{e,g} > 10^4$.

Equation (15) is used to obtain experimental values of the interfacial friction factor, $(f_i)_{exp}$, from the simultaneous measurements of the major flow parameters such as $\triangle P$, V_g, V_l and liquid depth along with flow geometries of A_g, S_g, S_i and L.

4.2. Measurements of Wave Characteristics for ε_i^*

In the gas-liquid stratified flow, f_i may be strongly influenced by the relative roughness of interface due to surface waves and the Reynolds number of the gas phase. The relative interface roughness, ε_i^*, on the other hand, is assumed to be given by Eq.(8):

$$\varepsilon_i^* \sim k\eta_o = \frac{2\pi}{\lambda}\eta_o \qquad (19)$$

In an effort to investigate the wave characteristics for ε_i^*, a total of 60 runs (i.e., 34 runs with a pipe test section and 26 runs with a duct test section) were made to measure the wave velocity (V_w), the wave length (λ), and the wave amplitude (η_o) at various flow rates of air and water in the wavy flow regime. In fact, these wave parameters were obtained during the measurements of major flow parameters to determine the $(f_i)_{exp}$. The results of the analysis of experimental data are briefly summarized here:

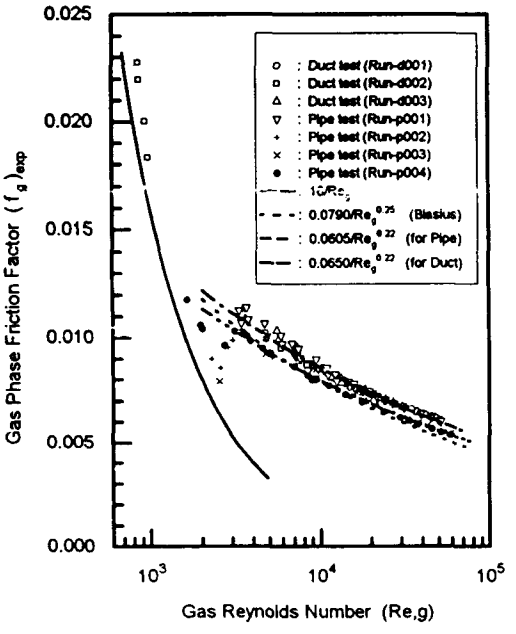

Fig. 3. Gas Phase Friction Factor for Pipe and duct Test Sections

(1) The wave velocity (V_w) versus the relative air velocity can be represented by

$$V_w = 0.042\ V_r + 0.12 \qquad (20)$$

Equation (20) shows that the wave velocity increases as the relative velocity is increased.

(2) In the wavy flow regime, the dimensionless wave length, λ/D, can be approximately expressed in terms of dimensionless velocity and the Reynolds number (based on V_r) as follows:

$$\frac{\lambda}{D} = 0.175\left(\frac{V_r}{\sqrt{gD}}\right)^{0.74} R_{e,r}^{0.1}\left(\frac{D_{h,l}}{D}\right) \qquad (21a)$$

where

$$R_{e,r} = \frac{V_r\ D_{h,g}}{\nu_g} \qquad (21b)$$

The plot of this curve, i.e., λ/D versus the right hand side of Eq.(21a) shows that the wave length λ varies from 0.3 to 2.5 times the pipe diameter (or hydraulic diameter) in the wavy flow regime. As the air velocity is increased, the flow regime changes from a wavy to a slug flow.

(3) As shown in Fig.4, in the wavy flow regime, the variation of the wave height to wave length ratio (η_o/λ) can be represented by

$$\frac{\eta_o}{\lambda} = 6.15\times10^{-4}\left(\frac{V_r}{\sqrt{gD}}\right)^{2/3} R_{e,r}^{1/3}\left(\frac{D_{h,l}}{D + D_{h,l}}\right)^{1/2} \qquad (22)$$

Since it is assumed that $\varepsilon_i^* = k\eta_o = 2\pi\eta_o/\lambda$, Eq. (22) implies that the relative roughness of the gas-liquid interface (ε_i^*) in a stratified wavy flow is approximately proportional to the first power of V_r (or V_g). As will be seen later, the functional form of the right hand side of Eq.(22) is the one that is used for the dimensionless velocity X in Eq.(9).

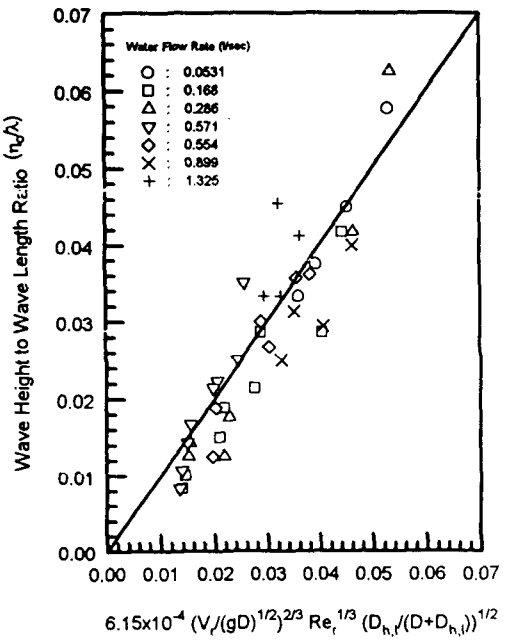

Fig. 4. Ratio of Wave Height to Length as a Function of Dimensionless Air Velocity in Wavy Flow Regime in a Duct Test

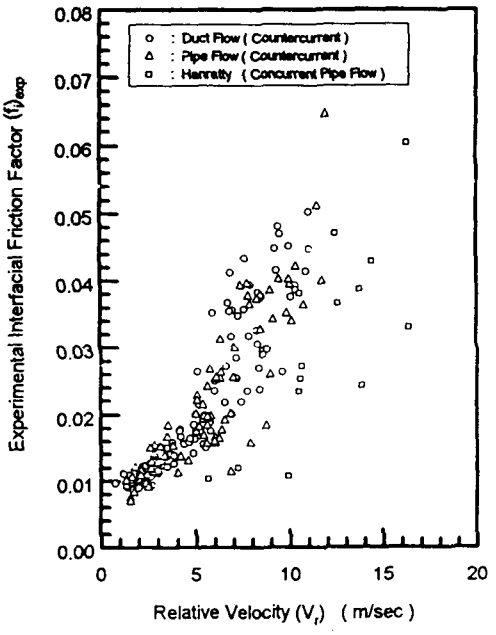

Fig. 5. Effect of Relative Velocity on $(f_i)_{exp}$

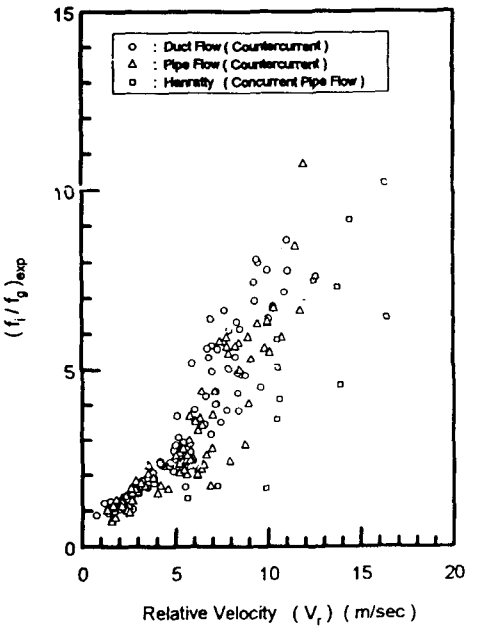

Fig. 6. Effect of Relative Velocity on $(f_i/f_g)_{exp}$

4.3. Effect of Major Flow Parameters on f_i

To examine the effect of major flow parameters on f_i, a total of 186 runs (i.e., 89 runs with a pipe test section and 97 runs with a duct test section) were made. The experimentally determined values of $(f_i)_{exp}$ and $(f_i/f_g)_{exp}$ are plotted against the relative velocity, V_r, in Figs.5, 6, and 7.

It should be noted here that both the water depth and the slope of the water level, in the present horizontal air-water countercurrent stratified flow, not only vary along the axial position of the test section but also depend on the velocity of the air V_g. Therefore, the air velocity used in the analysis is the mean value of the gas velocities calculated from the superficial gas velocity at the points where water depths are measured.

A brief summary of the effect of major flow parameters on f_i that can be found from Figs.5, 6, and 7 is as follows:

(1) Effect of V_r on $(f_i)_{exp}$ and $(f_i/f_g)_{exp}$: Figures 5 and 6 show that both $(f_i)_{exp}$ and $(f_i/f_g)_{exp}$ values in-

crease slowly with increase in the relative velocity until V_r reaches about $5m/s$, and beyond this point, both values increase more rapidly as V_r increases. Figure 6 shows that beyond $V_r = 5m/s$, $(f_i/f_g)_{exp}$ values jump from a value of about 3 to the maximum value of about 11 when $V_r = 12m/s$. This figure also shows that there are several data points where $(f_i/f_g)_{exp} < 1$. These data correspond to the cases where the liquid depth is high and V_r is extremely small (less than $2m/s$).

(2) Effect of Water Flow Rate on $(f_i)_{exp}$: To examine the effect of water flow rate on the $(f_i)_{exp}$, V_r versus $(f_i)_{exp}$ curves have been plotted for three different levels of water flow rate as shown in Fig.7. Although the water depth increases with increase in water flow rate, in general, the water depth does not vary linearly with water flow rate because of the dominant effect of air velocity. Figure 7 shows that when the relative velocity is higher than about $5m/s$, the interfacial friction factor increases with increase in the water flow rate for the same air velocity (or V_r).

From the above results, one may conclude that the most important flow parameter that influences the f_i is the gas velocity (or the relative velocity), and the next important parameter is the geometry of the liquid phase such as the liquid depth. The geometry

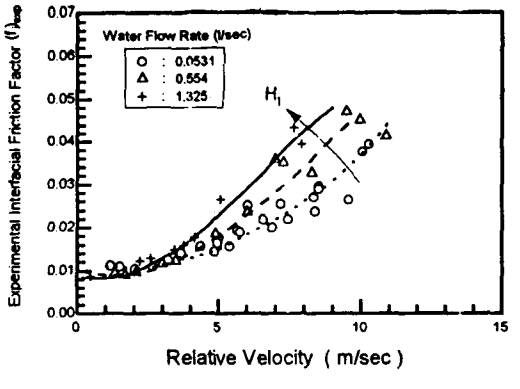

Fig. 7. Effect of Initial Water Flow Rate on $(f_i)_{exp}$ (Duct Test)

of the liquid phase, in the present work, is represented by the liquid hydraulic diameter $(D_{h,l})$ where the liquid depth enters as a parameter.

4.4. Final Correlation for f_i

The functional form for f_i as given by Eq.(9) is expressed in terms of a single dimensionless variable X and three constants. To determine the constants and X in Eq.(9), one cannot use a simple method of curve-fitting alone, because the dimensionless variable X appears also as an exponent in this equation. Therefore, a numerous repetition of trial and error has been used once the major parameters that contribute to the f_i values are identified in the foregoing analysis. That is, a number of different combinations of dimensionless variables have been tested against the present experimental data.

The final expression for f_i that gives the best agreement with the present experimental data is given by the following equations:

$$(f_i)_{corr} = 0.01(3X)^{(0.8+X)/4}$$

where

$$X = 0.02\left(\frac{V_r}{\sqrt{gD}}\right)^{2/3} R_{e,r}^{1/3}\left(\frac{D_{h,l}}{D + D_{h,l}}\right)^{1/2}$$

5. Summary and Conclusions

For the range of test parameters used in the present experiment, a semi-empirical correlation for the interfacial friction factor, based on the roughness in a wavy flow, can be expressed as Eqs.(23) and (24).

In Figs. 8 and 9, experimental values of the interfacial friction factor $(f_i)_{exp}$ obtained from both pipe and duct experiments are compared with those predicted by Eq.(23), $(f_i)_{corr}$. Typical existing concurrent flow data reported by Hanratty are also shown in Figs.8 and 9.

As can be seen in Fig.9, the agreement between the data and the predictions of the present correlation, Eq.(23), is within $\pm 30\%$. This result is fairly good considering that errors of more than $\pm 30\%$ are possible even in the predictions of two-phase flow pressure drop with well established existing

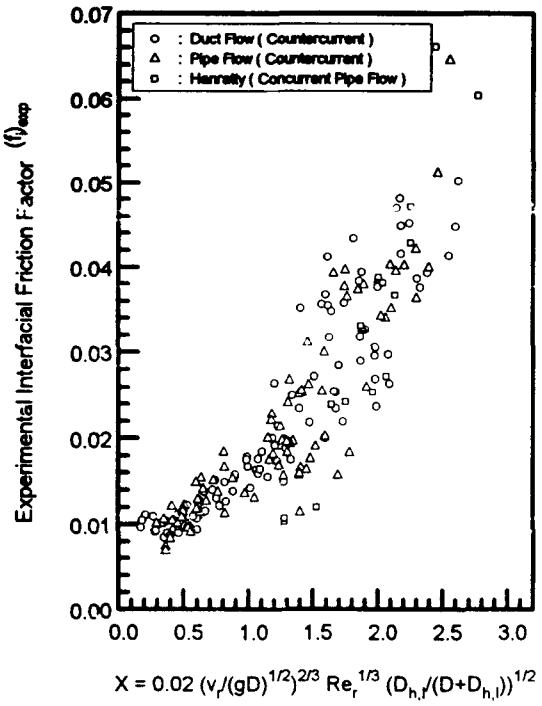

Fig. 8. $(f_i)_{exp}$ versus Dimensionless Velocity $\times$

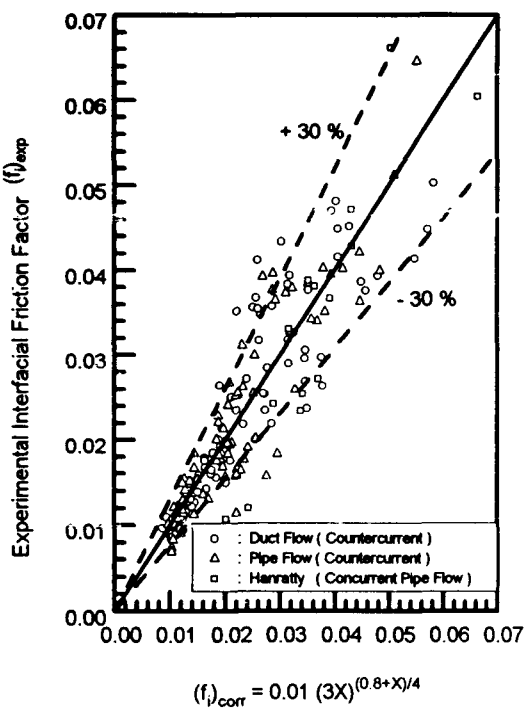

Fig. 9. Comparison of Experimental Values of $(f_i)_{exp}$ with Those Predicted by Present Correlation for Pipe and Duct Flow

correlations.

Thus, for the stratified wavy flow regime, the semi-empirical correlation developed in the present work can be used to predict the adiabatic interfacial friction factors in horizontal air-water countercurrent flow. In addition, the correlation proposed here can readily be incorporated in a computer code package which can provide the f_i values in the analysis of two-phase flow and system response, e.g., CIWH, two-phase pressure drop, and flooding.

Acknowledgement

Authors gratefully acknowledge the financial support of the Ministry of Science and Technology.

Nomenclature

A	flow area	m^2
a	a constant	
b	a constant	
c	a constant	
C_f	*skin-friction coefficient*	
D	diameter	m
f	friction factor	
g	gravitational acceleration, 9.80665	m^2
H	depth	m
L	length of pipe	m
m	mass flow rate	kg/s
P	pressure	Pa
R_e	Reynolds number	
S	perimeter	m
V	velocity	m/s
V_{gs}	superficial gas velocity ($V_{gs} \equiv m_g/\rho_g A$)	m/s
V_{ls}	superficial liquid velocity ($V_{ls} \equiv m_g/\rho_l A$)	m/s

V_w	wave velocity	m/s
X	dimensionless velocity	
x	axial position	m
Z	velocity	m/s

Greek Symbols

α	void fraction	*radians*
r	angle in Fig.2	m
ε	surface or interface roughness	m
η_o	wave amplitude or height	m
k	wave number	m^{-1}
λ	wave length	m
v	kinematic viscosity	m^2/s
ρ	density	kg/m^3
τ	shear stress	N/m^2

Subscripts

corr	correlation value
exp	experimental value
g	gas or steam
h	hydraulic
i	interfacial
ia	adiabatic interfacial
l	liquid
r	quantities defined in terms of relative value (V_r)
w	pipe wall

Superscripts

* dimensionless quantities

References

1. H.J. Kim, S.C. Lee, and S.G. Bankoff, *Int.* J. Multiphase Flow, 11(5), 593 (1985)
2. S.C. Lee and S.G. Bankoff, ASME *J. Heat Transfer*, 105, 713 (1983)
3. N.P. Cheremisinoff and E.J. Davis, *AIChE J.*, 25, 48 (1979)
4. M. Miya, D.E. Woodmansee, and T.J. Hanratty, *Chem. Eng. Sci.*, 26, 1915 (1971)
5. J.E. Kowalski, *AIChE Ann. Mtg.*, San Francisco (1984)
6. N. Andritsos and T.J. Hanratty, *AIChE J.*, 33(3), 444 (1987)
7. A.D. Altshul, Hand Book of Hydraulic Resistance (Edited by Idelchik, I.E.), Hemisphere, p.64 (1986)
8. H. Lamb, Hydrodynamics, Dover, p.455 (1945)
9. N. Andritsos and T.J. Hanratty, *Int. J. Multiphase Flow*, 13(5), 583 (1987)
10. L.F. Moody, *Trans. ASME*, 66, 671 (1944)